APPLICATION OF THE NASA AIRBORNE OCEANOGRAPHIC LIDAR TO THE MAPPING OF CHLOROPHYLL AND OTHER ORGANIC PIGMENTS

F. E. Hoge
NASA Wallops Flight Center
Wallops Island, Virginia

R. N. Swift
EG&G Washington Analytical Services Center, Inc.
Pocomoke City, Maryland

SUMMARY

This paper is intended to review laser fluorosensing techniques used for the airborne measurement of chlorophyll *a* and other naturally occurring waterborne pigments. Previous experiments demonstrating the utility of the Airborne Oceanographic Lidar (AOL) for assessment of various marine parameters are briefly discussed. The configuration of the AOL during the NOAA/NASA Superflux Experiments is described. The participation of the AOL in these experiments is presented and the preliminary results are discussed. This discussion centers on the importance of multispectral receiving capability in a laser fluorosensing system for providing reproducible measurements over wide areas having spatial variations in water column transmittance properties. This capability minimizes the number of truthing points required and is usable even in shallow estaurine areas where resuspension of bottom sediment is common. Finally, problems encountered on the Superflux missions and the resulting limitations on the AOL data sets are addressed and feasible solutions to these problems are provided.

INTRODUCTION

The NASA Wallops Flight Center (WFC) Airborne Oceanographic Lidar (AOL) participated in two series of field experiments conducted within the joint NOAA/NASA Superflux Study. During these experiments the AOL was flown onboard the WFC P-3A aircraft together with the Langley Research Center (LaRC) Multichannel Ocean Color Scanner (MOCS), L-band microwave radiometer, Test Bed Airborne Multispectral Scanner (TBAMS), and Airborne Lidar Oceanographic Probing Experiment (ALOPE) systems. The first series of Superflux missions was flown between March 17 and 19, 1980, while the second series was flown between June 20 and 27, 1980. Although all data sets have been reduced and have received preliminary analysis only those results from the June experiments are reported here and are hereafter labeled as WFC AOL Mission numbers 30, 31, 32 and 33.

These sensor systems formed a reasonably complementary group. The MOCS and TBAMS are passive multispectral scanners which can be directly analyzed with the active AOL multispectral system and can possibly be used to extend the utility of the lidar results which were acquired in a profiling mode. However, both of the passive sensors are ideally operated at a much higher altitude than 150 m and most of the passive data were obtained on separate missions. The L-band radiometer is a passive microwave sensor capable of determining the salinity of the surface water layer. The salinity information from the L-band radiometer together with thermal data from a Precision Radiometric Thermometer Model PRT-5 infrared sensor (recorded independently by the AOL and ALOPE systems) can be utilized to establish the physical framework necessary for ultimately interpreting the results of the optical sensors. The ALOPE, like the AOL, is a laser fluorosensing system but differs in that it utilizes two (and potentially four) laser wavelengths for excitation and has only a single channel receiver capability. The dual wavelength stimulation of the ALOPE system makes the recovery of relative concentrations of various phytoplankton color groups possible while the multispectral receiver capability of the AOL allows correction for spatial variations in water transmissivity properties through normalization with the 3400 cm^{-1} water Raman backscatter signal.

One of the most important objectives of the Superflux missions was to present an opportunity for testing various NASA remote sensing systems to meet NOAA/NMFS data acquisition requirements related to providing an initial baseline data set and future monitoring of Atlantic coastal waters. Further, these missions afforded NASA an opportunity to test its remote sensors in experiments where a number of surface truthing vessels were available and coordinated. Key to the joint program is the recognition by all that oceanic data acquisition requirements cannot be achieved using conventional techniques alone. Assessment goals can only be reached through extensive use of remote sensors (both airborne and spaceborne) and the prudent application of expensive conventional techniques to extend the reliable coverage of these remote sensors. The Superflux program seeks not only to determine the feasibility of remote sensing parameters of interest that can be directly measured by the sensors themselves, but also to evaluate the degree to which associated parameters (that are not directly measured by these sensors) can be reliably determined or inferred. Since the AOL has numerous potential applications beyond those demonstrated on the Superflux missions but which are likewise pertinent to the future NMFS assessment program, we have included a brief review of these capabilities as part of this paper.

The use of laser-induced water Raman backscatter for oil film detection and thickness measurement was demonstrated with the AOL over EPA-approved oil slicks in a series of experiments conducted in 1978. A 337.1-nm nitrogen laser was used to excite the 3400-cm^{-1} OH stretch band of natural ocean water beneath the oil slicks from an altitude of 150 m.[1] The signal strength of the 381-nm water Raman backscatter was always observed to decrease when the oil was encountered and then return to its original value after complete aircraft traversal of the floating slick. After removal of background and oil fluorescence contributions the ratio of the depressed-to-undepressed airborne

water Raman signal intensities, together with laboratory-measured oil extinction coefficients, was used to calculate the oil film thickness. In addition, analytical work currently ongoing at WFC indicates that thickness may also be recovered from airborne laser-induced fluorescence from the oil. Oil spill type classification or fingerprinting data analytical efforts are in progress using absolute oil fluorescence conversion efficiency techniques.

The measurement of the concentration of a fluorescent dye deployed in open ocean water was demonstrated with the AOL using similar techniques.[2] Since the amplitude of the Raman signal is directly proportional to the volume of water being accessed by the laser pulse, the amplitude of the fluorescence return varies directly as the number of dye molecules in that volume. In turbid waters only the very surface may be sampled and hence only high concentrations can be detected; whereas lower concentrations can be observed in clear water with significantly deeper beam penetration. Concentrations of Rhodamine WT dye (frequently used as a tag during circulation experiments) were measured to 2 ppb during field tests conducted in 1978.

The simultaneous measurement of Raman backscatter, chlorophyll *a*, and other naturally occurring pigments was demonstrated using the AOL in 1979 during experiments conducted in the German Bight and in estuarine waters in the vicinity of WFC.[3] These field experiments utilized essentially the same instrument configuration and technology reviewed in this paper, however the operation of the fluorosensor was improved and available surface truthing support was much better during the Superflux experiments, potentially allowing the Superflux results to be of greater analytical utility to marine scientists.

The feasibility of performing bathymetric measurements to depths of up to 10 m with an airborne lidar system was demonstrated using the AOL in a joint NASA/NOAA/NORDA program conducted in 1977.[4] The potential importance of this work to the future NMFS program would be the application of this previously developed depth resolution capability to resolving the vertical distribution of various fluorescent parameters such as chlorophyll *a*.[2,3]

INSTRUMENT DESCRIPTION

The Airborne Oceanographic Lidar (AOL) is a state-of-the-art scanning laser radar system having a multispectral time-gated receiving capability. The system is designed to allow adjustment in most transmitter and receiver settings. This built-in flexibility gives the AOL system potential application in many oceanographic areas. Portions of the hardware and software capabilities of the AOL have been briefly discussed elsewhere[1-5] but will be summarized and expanded as needed to illustrate the important aspects of the fluorosensing mode of the instrument as utilized during the Superflux experiments. Figures 1 and 2 should be consulted during this hardware description. Figure 2 is a detailed portion of the AOL spectrometer whose location in the system is given within Figure 1.

The AOL was operated in the fluorosensing mode during all of the Superflux missions. The AOL system laser (Avco Model C-5000) was entirely replaced with a frequency-doubled Nd:YAG laser having a 532.1-nm output wavelength. A high speed silicon photodiode viewed radiation extraneously scattered from the first folding mirror to provide the start pulse timing and monitoring of the analog output pulse power signal. Digitization and recording of this signal allow the data to be corrected for laser output power variations. The pulsed laser output is folded twice through 90° in the horizontal plane of the upper tier into the adjustable beam divergence/collimating lens. The laser output beam divergence of the frequency-doubled YAG laser is controllable only between 0.3 and 5 mrad. Minimum divergence was used during all of these field experiments. The beam is then folded directly downward through the main receiver folding flat, finally striking the angle-adjustable nutating scan mirror. The scan mirror is 56 cm in diameter and is connected at its center in a wheel-and-axle type configuration. This mirror is integrally connected with an adjustable concentric counterbalance wheel so that the entire mechanism does not vibrate when the mirror is rotated in nonperpendicular positions of 5, 10, or 15°. A setting of 15° off nadir was used for all Superflux missions and the data were obtained in a nonscanning mode. This scan mirror finally directs the beam to the ocean surface. The total surface, volume, and/or ocean bottom backscattered signals return through the same path but because of their uncollimated spatial extent are principally directed into the 30.5-cm Cassegrainian receiving telescope. The horizontal and vertical fields of view of the receiving telescope are each separately controlled by a pair of operator-adjustable focal plane knife-edges. The radiation is then collimated to eliminate undesirable skewing of the bandpass by subsequent narrowband interference filters. The radiation is then focused 3 cm behind the face of the EMI D-279 PMT to avoid weak photocathode areas. The combination 45° folding flat and beam splitter located between the collimating lenses and the narrowband interference filter is used only in the fluorosensing mode.

The beam-splitting mirror directs a major portion of the excitation wavelength and the fluorescent return signal into the fluorosensing detector assembly. The YAG laser excitation wavelength (532 nm) component of the return signal was rejected from the spectrometer by a Kodak 21 high-pass (wavelength) filter. This filter rejects radiation below 540 nm. A small amount of the surface return signal is allowed to pass through a small 1-cm opening in the beam splitter where it is sensed by the bathymetry photomultiplier tube and subsequently used to measure slant range and to generate the gate pulses for the analog-to-digital charge digitizers (CD). A 0.3-nm narrowband interference filter was placed into the 11-cm diameter collimated return beam just behind the beam splitter. The bathymetry photomultiplier tube portion of the system must therefore function during all modes of operation and slant range information is available at all times.

The fluorosensing detection assembly contains an 11-cm diameter transmission diffraction grating blazed for 480.0 nm having 600 grooves/mm. An 11-cm diameter simple lens brings the dispersed radiation to the entrance surface of thirty-six quartz light guides. These guides are optically coupled to two separate banks of 20 RCA C71042 phototubes of which a total of only thirty-six were used in these experiments. The front faces of the light guides are

physically located in the focal plane to receive the dispersed spectral components nominally from 390 to 800 nm. This configuration yields a spectral bandwidth of 11.25 nm for each channel. The tubes are not shuttered or gated but remain active at all times. Ambient background radiation rejection is provided by the 0-20 mrad adjustable field-of-view (FOV) knife-edge pairs located at the focal point of the receiving telescope. The optimum operational FOV for our field tests was experimentally determined to be 4 mrad by observing the water Raman SNR. The pulsed analog outputs of the entire bank of phototubes are routed to ac-coupled buffer amplifiers that drive each of the thirty-six charge digitizer (CD) input channels. The amplifiers respond only to wide bandwidth fluorescent pulses, and thus response to background noise is very minimal permitting full daylight operation.

The fluorosensor PMT analog outputs are routed through 10X buffer amplifiers and digitized. All thirty-six charge digitizers are simultaneously gated ON to obtain the entire spectral waveform at a temporal position determined by the surface return signal from the bathymetry photomultiplier tube. Additionally, the CDs can be held ON for selectable integration times of 15 to 150 nsec using a LeCroy model 161 discriminator. An integration period of approximately 30 nsec was used during all of the Superflux missions. The CDs are fundamentally the analog-to-digital converters for the AOL spectral waveform digitizing system. The charge digitizers are 10 bit yielding a maximum of 1024 counts. Their output is directed through CAMAC standard instrumentation to a Hewlett-Packard 21MX computer for recording. With proper delay adjustments relative to the bathymetry PMT-derived surface return, the spectral waveforms may be taken at any position above or below the ocean surface. In this experiment the spectral waveform data acquisition was started 3 nsec prior to encountering the surface and terminated 30 nsec later. Summary information and additional instrumentation details may be found in Refs. 1 through 4.

DESCRIPTION OF THE FIELD WORK

During the June 1980 Superflux field experiments the AOL was flown on five separate missions, however the first mission of this series was flown near the mouth of the Delaware Bay and is not included in this paper. Figures 3 and 4 are computer plots of the flightlines occupied on the remaining four missions. The purposes of the AOL participation in these missions were (1) to assess the precision and accuracy of the system in providing total chlorophyll *a* concentration in the surface layer (upper 5 m) of water column, and (2) to provide wide area, nearly synoptic maps of the distribution of water transmissivity and chlorophyll *a* concentration (as well as the relative distribution of other organic pigments) in the vicinity of the Chesapeake Bay mouth and adjacent Atlantic shelf. Further, the AOL was used to digitally record the analog output of the PRT-5 infrared thermal sensor.

The flightlines were arranged primarily to provide wide areal coverage of the study area with convergence and closer spacing around the vicinity of Cape Henry where spatial gradients of the various parameters were expected to be the most pronounced. On some of the missions however certain of the flightlines were repeated or arranged in a crossing pattern. Although the repeating lines do not appear to provide optimal use of prime flight time they do provide an effective measure of precision and repeatability for an unproven sensor as will be seen in the succeeding section of this paper. Likewise, crossing or highly converging lines can be used to assess the internal consistency of a sensor provided the temporal separation between the lines is short relative to the temporal flux in parameter concentrations. Once the precision of the sensor is documented, however, the crossing lines having larger temporal separation can be used to infer dynamic changes in parameters. Unfortunately available flight time did not permit the inclusion of many repeating or crossing lines.

The surface truthing logistics were coordinated by the LaRC experiment team. On each mission various research vessels were deployed at points designed to be coincident with the projected ground track of the P-3 aircraft. The results of surface measurements taken at these points would then serve as standards against which to test the accuracy of the onboard sensors and these measurements would subsequently allow the relative values obtained by the sensors to be converted into absolute concentrations. Once converted, the airborne sensors allow extension of the reliable surface measurements over wide areas in a reasonably synoptic manner. The utility of this technique is of course dependent on the ship's sampling the same watermass that was observed by the sensor. Temporal and spatial separation between airborne and surface sampling degrades the confidence that can be attached to the sensor data. In practice, perfect sampling coincidence is nearly impossible, therefore the relative variation in the gradients of the constituents under consideration both in time and space must be taken into account in assessing the degree of reliability to be attached to the sensor testing. This topic will be expanded in the concluding portion of the next section of this paper.

DISCUSSION OF RESULTS

This section has been divided into subsections in order to pursue discussion of several separate but related aspects of the AOL participation in the Superflux experiments. The initial subsection describes the multispectral data obtained by the AOL, the second portion of this section examines the necessity for applying corrections to the spectra for spatial variations in the transmissivity properties of the water column, and the final section examines the degree of confidence that can be placed on the AOL data obtained during the Superflux experiments. The results presented herein must be considered preliminary in that more analysis will be required before it will be a fully functional data set. As will be pointed out in the succeeding discussion, there are additional corrections to be made to the data with regard

to adjusting the spectral waveform. Beyond this there are some inherent errors for which we will not be able to compensate. These errors do not appear to seriously degrade the utility of the AOL results. Feasible solutions to these remaining problems will be presented and most of these solutions are either in the process of being implemented or can be effected by the time the next mission of this type is undertaken. The logistical difficulties described in the final portion of this section should not be construed as criticism of the experiment team but rather as suggestions for improving future efforts.

AOL Data Description

The 532.1-nm excitation wavelength provided by the frequency-doubled YAG laser yields spectra similar to those obtained from Chesapeake Bay water in work performed at the Langley Research Center (LaRC) laboratories.[6] Similar spectra were obtained by the airborne lidar system (AOL) on the Superflux experiments. Compare the laser-induced spectra obtained within the bay plume (Figure 5a) with one obtained offshore (Figure 5b). The locations of these sampling points are noted on Figure 4. Each airborne spectrum is a simple average of five seconds of data gathered at 6.25 pps or 31 waveforms. The three spectral lines of most interest are labeled in both Figures 5a and 5b. These spectral peaks correspond to the Raman backscatter, chlorophyll _a_, and organic pigment lines at 645 nm, 685 nm, and 580 nm respectively. The organic pigment line has not been fully understood and is currently being investigated in joint WFC/LaRC experiments. Openings were provided through the longpass filter to allow a small amount of on-wavelength backscatter into the spectrometer at 532 nm. These spectra have not been corrected for a slight distortion from the Kodak 21 longpass filter used to partially reject the laser wavelength from the spectra. Also, cross-channel interference between the Raman peak return and the chlorophyll _a_ return have not been deconvolved. This may produce some error in both very clear, offshore waters where our relative chlorophyll values may be slightly elevated or in turbid, nearshore waters with strong chlorophyll responses where our relative chlorophyll values may be too low.

In analytical work performed on the Superflux data sets at WFC we have produced a number of data products that we feel will be useful in interpreting the results of the field experiments and in preparing technical papers some of which are planned for joint authorship with other Superflux investigators. These products include time-series cross-sections and spatial contour plots of pigment, Raman, and chlorophyll _a_ spectral peaks. The time-series cross-sectional projections have been prepared for all passes taken during the Superflux experiment while the contoured projections have been produced only for the missions flown on June 23, 25 and 27, 1980. The mission flown on June 20th had too few flightlines to allow contouring. Figure 6 is an example of a cross-section from a pass flown on June 23rd and is typical of the plots obtained on most of the passes flown within the bay or across the bay outflow plume. Note the large increase in chlorophyll _a_ as the mouth of the bay is approached during the latter portion of the flightline. The actual location of this flightline 4 is given in Figure 3b. Figures 7-9 are individual contour plots of Raman, chlorophyll _a_ and pigment produced from the mission flown on June 23. The dotted segments indicate the actual aircraft flight ground tracks. Note that the Raman values vary inversely with attenuation, thus the higher Raman values on these

plots represent clearer water while the lower values indicate more turbidity in the upper layer of the water column. Of particular interest are the distribution of clear and turbid watermasses on the Raman contour plot and the presence of the outflow plume evident on all three contour plots. The contour plot in Figure 7 has been corrected only for altitude and laser power variations. Contour plots 8 and 9 have been corrected for altitude, laser power fluctuations, and spatial variations in the optical properties of the watermass. This latter correction has been made to the organic pigments and chlorophyll *a* response peaks by normalization with the water Raman response peak of Figure 7. This normalization procedure will be discussed in detail in the next subsection. The cross-sections as well as the contoured projections made from them are presently relative parameter values comparable only to other parameter values taken within the same data set. Through the application of available truth measurements it appears that the AOL chlorophyll *a* fluorescence data can be converted into absolute units of concentration on at least three of the four Superflux missions. This will be discussed subsequently. As we shall see, the truth data from Figure 12b can be used to convert Figure 8 to an absolute chlorophyll *a* concentration map.

Three major problems remain in the AOL Superflux data sets. These are (1) spectral distortion from the Kodak 21 filter; (2) separation of Gelbstoff fluorescence from that of the other organic pigments; and (3) the spectral overlap of the water Raman backscatter and chlorophyll *a* fluorescence signals. Correction for the Kodak 21 filter appears to be the least significant of these difficulties. The spectral properties of this filter are well known and thus corrections for distortion can be applied in a straightforward manner. The other two problems are more difficult to address. The separation of Gelbstoff fluorescence from the responses of the other organic pigments cannot be fully addressed in the Superflux data sets and will likely not be attempted. The problems due to spectral overlap of the chlorophyll *a* and Raman signals can be corrected for the most part through interpolation techniques similar to those presented in Reference 1. As will be shown in the final portion of this section, this latter problem does not appear to present a serious error in the Superflux data sets where the total chlorophyll *a* concentration primarily remained between 0.2 and 5.0 μg/ℓ. This error, however, would become significant in conditions of high total chlorophyll *a* concentration.

The solution to both of these latter problems appears to involve a shift in the laser wavelength. A field study aimed at resolving both the photo-pigments and chlorophyll might best be addressed by using a fluorosensing system equipped with two laser wavelengths. One laser could be operated at a wavelength in the 515-520 nm region. This excitation wavelength would place the Raman backscatter line in the 620- to 628-nm portion of the spectrum, thus providing a reasonable separation from the chlorophyll line at 685 nm. The other laser could be a nitrogen system at 337.1-nm excitation wavelength allowing better definition of the broad Gelbstoff response. These lasers could be alternately pulsed or be used one at a time on alternating passes made over the same flightline.

Corrections for Spatial Variations in Water Transmissivity Properties

The importance in laser fluorosensing of applying corrections to the various fluorescence responses for spatial variation in water column transmittance properties cannot be overstressed for the precise recovery of even relative concentrations of various parameters. The transmittance of the water can be measured from the participating surface truth vessels using in situ techniques for recovering α and K, the beam and diffuse attenuation coefficients respectively. Alternately, the "apparent" transmissivity of the water can be directly acquired by the laser fluorosensor itself by monitoring the 3400 cm^{-1} water Raman backscatter signal. The Raman backscatter signal is proportional to the number of water molecules accessed by the laser pulse during the receiver integration period. If the Raman line is sufficiently close to the response line of the parameter to be corrected the relative concentration of that parameter can be found by simply normalizing its response intensity with that of the water Raman. This technique has been recently demonstrated with a dual channel receiver[7,8] using a 50/50 beam splitter and respectively isolating the Raman and chlorophyll *a* lines with a 10-nm interference filter centered at 560 nm and a 23-nm filter centered at 685 nm. A dual channel receiving system is however restricted to monitoring single parameters and necessarily the resulting data cannot be corrected for spectral interference from other responses such as described in the preceding section. Further, with increasing importance potentially attached to other fluorescence response wavelengths[6,9,10] we feel that a multichannel receiving capability is the appropriate type sensor for baseline assessment and monitoring in estuarine and nearshore water bodies.

Figure 10 illustrates the importance of the normalization procedure. The cross sections shown in Figure 10 are time history plots of the peak channel amplitudes of the organic pigment, Raman, and chlorophyll *a* lines for Pass 8 of the Superflux mission flown on June 27, 1981. The location of Pass 8 is shown in Figure 4. The chlorophyll *a* and pigment profiles in Figure 10a have not been normalized with the water Raman data. In Figure 10b the chlorophyll *a* and pigment peak values have been divided (or normalized) by the corresponding 645-nm Raman peak obtained simultaneously. The amplitude of the Raman peak channel is of course not normalized and remains the same in both Figure 10a and Figure 10b. The Raman cross section is representative of the relative water transmissivity and thus increases in amplitude in areas of clearer water and correspondingly lowers in amplitude in areas of more turbid water. As expected, the Raman cross section indicates that the offshore water is more transmissive than the water just off Cape Henry where the flightline was discontinued. Notice that the raw chlorophyll *a* and organic pigment responses appear to only increase slightly over the flightline on Figure 10a. In Figure 10b however, the corrected responses of both the chlorophyll and organic pigments are decreased from their previous values offshore where the Raman signal indicates a larger volume of water was accessed by the laser pulse. They are larger nearshore in the more turbid watermass where a smaller volume of water was accessed as indicated by the lower Raman signal.

Most of the flightlines flown during the Superflux experiments had variations in the spatial distribution of water transmittance similar to that shown in Figure 10. Patchiness in water clarity and chlorophyll concentration was especially evident within the bay proper and in the bay outflow flanking the Virginia shoreline south of Cape Henry. We have found these variations typical of most watermasses overflown within the Chesapeake and Delaware Bays, on the Atlantic shelf, and in the German Bight of the North Sea.

Results of AOL Self-Consistency Tests and Comparison with Surface Truth Measurements

The internal consistency and precision of the AOL can be adequately demonstrated by the reoccupation of flightlines within short time intervals or by flying a grid pattern of flightlines with many crossing points. Of the two options available we prefer the reoccupation of the same line since this procedure furnishes considerably more overlapping points, temporal separation between overlapping points can be minimized, and uncertainties in positioning as determined by the onboard Litton LTN-51 Inertial Navigation System (INS) or the auxiliary Loran-C system are reduced. The crossing grid pattern, on the other hand, allows maximum areal coverage while still presenting enough overlapping points to insure that no drift in the AOL system has taken place.

During the course of the Superflux experiments a number of lines were reoccupied during the same experiment. Of these data sets, however, only Passes 6 and 16 of the mission flown on June 27th are usable for testing sensor precision. The locations and flight directions of Passes 6 and 16 are labeled in Figure 4b. The remaining sets were either monotonous (located too far offshore or too far south of Cape Henry), had gross temporal separation, or in one case the set was flown at the very beginning of a mission when the AOL was still being adjusted and optimized.

Cross-sectional plots of Passes 6 and 16 are shown on Figure 11. The three parameters (chlorophyll, Raman, and pigment) of interest are labeled in the figure. The two passes were flown in opposite direction with respect to one another. The chlorophyll and pigment responses have been normalized with the Raman backscatter signal. Note the agreement in all cases, even down to relatively small-scale features. At this point we have not attempted to statistically quantify the agreement although it is our intention to do so as we continue our analysis of Superflux data.

Although only one set of passes can be compared in this manner from the Chesapeake Bay Superflux missions we have been able to compare three sets of passes from the Delaware Bay Superflux mission (June 1980) and two sets from missions flown in the German Bight area of the North Sea (1979).[3] All of these comparisons have been favorable indicating that the internal consistency of the AOL is dependable from mission to mission and over a time frame of one year.

Surface truth samples are not only useful for proving the accuracy of the AOL but are also required to allow extrapolation of absolute chlorophyll concentrations from the relative values of corrected chlorophyll backscatter signal available from the pre-processed AOL data. The agreement between the AOL and surface truth chlorophyll measurements then affects both the absolute concentration values and the degree of confidence that can be placed on the AOL results. During the Superflux experiments an attempt was made to place the surface truth vessels at points that were coincident with an intended overpass as nearly in both time and space as possible. As will be subsequently shown, considerable spatial and temporal differences between airborne observations and surface truth measurements were experienced. Fortunately, reasonable agreement between the AOL and surface truth chlorophyll determinations was found during the analysis of the four Superflux missions flown in June. However, this sampling disparity is a limiting factor on both the instrument credibility and the confidence with which oceanographers can apply the AOL results.

Figure 12 shows the comparison between the AOL and surface truth chlorophyll results for all four Superflux missions conducted during June 1980. All available surface truth samples occurring within one nautical mile or within 60 minutes of an airborne observation were used in this comparison. The positions of both the surface vessels and the aircraft were obtained from their respective Loran-C receivers. A computer program was used to pick the particular AOL sample spatially nearest the surface truth observation within the arbitrarily chosen one hour time constraint. For the sampling points located well offshore both the temporal and spatial constraints were relaxed. Linear correlation coefficients determined for each of the four missions are given within their respective plots. In general, we consider the agreement reasonably good over the entire range of chlorophyll concentration with the exception of some minor disagreement found during Mission 32. The slopes are somewhat varied from mission to mission because of variations in the fluorosensor gain caused by using a different PMT high voltage setting. Also, the placement of the spectrum within the 36 fluorosensor light guides was sometimes varied from mission to mission. The placement of the spectrum upon the light guides can be adjusted by angular movement of the plane of the beamsplitting mirror immediately in front of the bathymetry PMT. The plane of this mirror was changed from mission to mission during these experiments in an attempt to optimize the spectral response of the AOL. More recent techniques in pre-flight preparation of the instrumentation and hardware improvements are expected to result in better fluorosensor spectra and considerably lower mission-to-mission variability in gain and bias.

Logistical planning and sampling coordination between airborne sensors and surface truthing vessels play a vital role in the ultimate usefulness of data from experiments such as Superflux. It is therefore worth examining the sampling coordination experienced during these experiments for utility in planning future experiments. Plots of temporal and spatial differences between airborne and surface truth sampling are given in Figure 13 for the respective passes discussed above. Although time and space cannot be equated in such a straightforward fashion for gauging the probable effects on the results of the intercomparisons, the general spread of differences between surface and airborne sampling on all

missions does indicate a significant possibility that some of these samples were extracted from different naturally occurring populations. It should be noted that, in general, those points indicating the largest differences represent offshore measurements where coincident sampling is least important. Also, the distribution of sampling differences on the plot for Mission 32, which had the poorest agreement on the regression analysis, is not much different than the distributions shown for the other missions. Perhaps this lack of agreement is due at least in part to the effect of the tidal phase in which the sampling was conducted. Mission 32 was flown during the flood cycle while the remaining missions were flown during the ebb cycle or near slack water. The higher vertical turbulence of the flood tide has been well documented as has the patchiness of various entrained parameters during that tidal cycle. This increased turbulence and attendant patchy distribution of chlorophyll and particulate matter would tend to magnify the effects of sampling differences.

The other aspect of coordinated surface and airborne sampling that appears to have been important during the Superflux experiments is the local gradient of various parameters in the vicinity of the sampling points. Figures 14 and 15 are time series cross-sections of normalized chlorophyll for passes flown during Mission 32 from which a comparative sample(s) was extracted for the preceding intercomparison. The location of the sampling point(s) on each pass is indicated by small arrows placed above the profile. The potential difference in values that could result from rather small horizontal displacement between aircraft and surface vessel sampling positions is especially apparent on Figure 15 while the lower gradients shown on Figure 14 would result in much lower potential differences. Attention should be afforded to this aspect on future missions, however it is realized that patchiness is almost an inherent problem in "high" chlorophyll areas within dynamic estuarine systems such as the lower Chesapeake Bay.

SUMMARY AND CONCLUSIONS

The results of the AOL flight tests conducted during the Superflux Experiments indicate that rapid, synoptic assessment of surface layer concentrations of chlorophyll and related pigments is feasible from an airborne laser fluorosensing system. Further, these initial tests show that the lidar system provides repeatable results with high internal consistency. Several problems have been identified in the present data set. As previously discussed the data presented herein has not been corrected for the effects of the Kodak 21 filter, the Gelbstoff component has not been separated from other fluorescent returns in the 580-nm region of the spectrum, and cross talk (caused by the low 11.25-nm AOL resolution) between the Raman and chlorophyll returns has not been deconvolved. Nevertheless, the results indicate that stimulation of natural waters with 532-nm wavelength radiation will (1) yield good results for chlorophyll concentrations ranging from 0.2 to 5 μg/ℓ, (2) provide satisfactory but not ideal Raman placement for correction of water attenuation properties, and (3) probably yield Gelbstoff fluorescence potentially mixed in an ambiguous combination with fresh biological photo-pigments.

The results of intercomparisons made between the AOL and surface truth chlorophyll measurements appear to be reasonably good with linear correlation coefficients varying between 0.81 and 0.97. Further, these comparative plots appear to have a linear fit through the distribution of points indicating that the spectral overlap of the Raman and chlorophyll has not seriously degraded the AOL chlorophyll results for the concentrations encountered in these field studies. Some problems associated with the coordination of aircraft and surface vessel sampling were discussed in the preceding section of this paper, but with the possible exception of Mission 32 the spatial and temporal disparities in coincident sampling do not appear to have produced a serious effect on the agreement between AOL and surface truth measurements of chlorophyll. However, these problems should be addressed in planning future missions of this type. Conversion of the AOL relative chlorophyll values to absolute concentration values using the slopes calculated in the linear regression analysis is practical in view of these results. Contour and cross-sectional projections of this data can be utilized by the oceanographer with reasonable confidence.

AOL hardware and software changes currently being implemented should provide improvements to the spectral problems discussed in the preceding section and are expected to significantly reduce the mission-to-mission variability experienced during the Superflux missions. The addition of a second laser wavelength (a) should also allow separation of some phytoplankton color groups as has been demonstrated with the LaRC ALOPE laser fluorosensor and (b) may facilitate the separation of Gelbstoff fluorescence from that of other organic pigments.

REFERENCES

1. Hoge, F. E.; and Swift, R. N.: Oil Film Thickness Measurement Using Airborne Laser-Induced Water Raman Backscatter. Appl. Opt., vol. 19, no. 19, 1980, p. 3269.

2. Hoge, F. E.; and Swift, R. N.: Absolute Tracer Dye Concentration Using Airborne Laser-Induced Water Raman Backscatter. Appl. Opt., vol. 20, no. 7, 1981, pp. 1191-1202.

3. Hoge, F. E.; and Swift, R. N.: Airborne Simultaneous Spectroscopic Detection of Laser-Induced Raman Backscatter and Fluorescence from Chlorophyll and Other Naturally Occurring Pigments. Appl. Opt., vol. 20, no. 18, 1981.

4. Hoge, F. E.; Swift, R. N.; and Frederick, E. B.: Water Depth Measurement Using an Airborne Pulsed Neon Laser System. Appl. Opt., vol. 19, no. 6, 1980, pp. 871-883.

5. Bressel, C.; Itzkan, I.; and Nunes, J. E.; and Hoge, F. E.: Airborne Oceanographic Lidar System. Proceedings, Eleventh International Symposium on Remote Sensing of the Environment, vol. 2, Environmental Research Institute of Michigan, Ann Arbor, 1977, pp. 1259-1268.

6. Zimmerman, A. V.; Paul, Fred W.; and Exton, R. J.: Research and Investigation of the Radiation Induced by a Laser Beam Incident on Sea Water. NASA CR-145149, 1976.

7. Bristow, M.; Nielsen, D.; Bundy, D.; Furtek, R.; and Baker, J.: Airborne Laser Fluorosensing of Surface Water Chlorophyll a. U.S. Environmental Protection Agency, Report no. 600/4-79-048. 1979.

8. Bristow, M.; Nielsen, D.; and Furtek, R.: A Laser-Fluorosensor Technique for Water Quality Assessment. Proceedings, Thirteenth International Symposium on the Remote Sensing of the Environment, vol. 1, Environmental Research Institute of Michigan, Ann Arbor, 1979, pp. 397-417.

9. Zimmerman, A. V.; and Bandy, Alan R.: The Application of Laser Raman Scattering to Remote Sensing of Salinity and Turbidity. Final Technical Report, Contract NAS1-11707 (Task 33), Old Dominion University Research Foundation, Norfolk, Virginia, 1975.

10. Bristow, M.; and Nielsen, D.: Remote Monitoring of Organic Carbon in Surface Waters. Project Report no. EPA-600-4-81-001, U.S. Environmental Protection Agency, 1981.

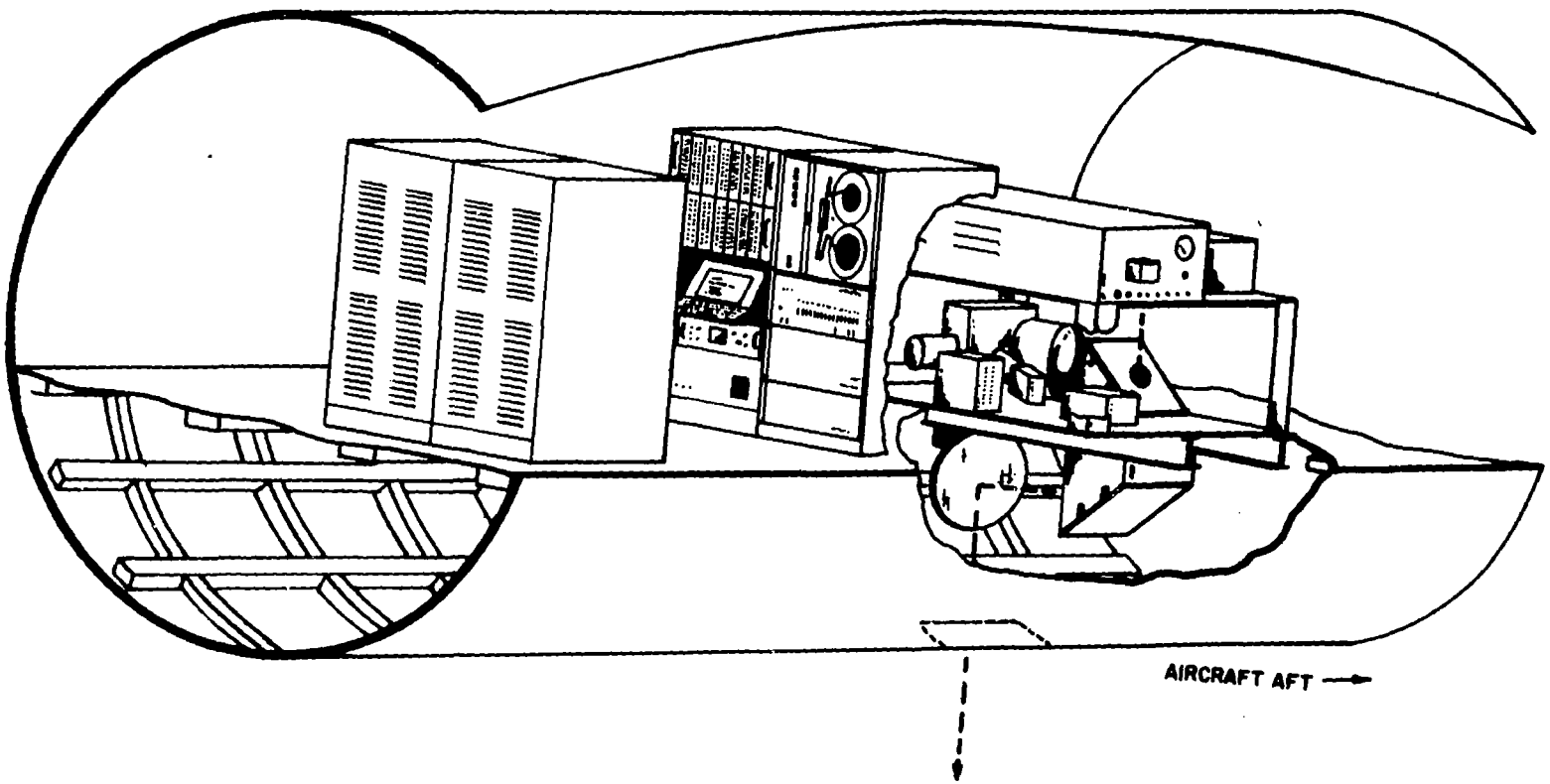

Figure 1.- Cut-away view of the AOL system as arranged on the WFC P-3 aircraft.

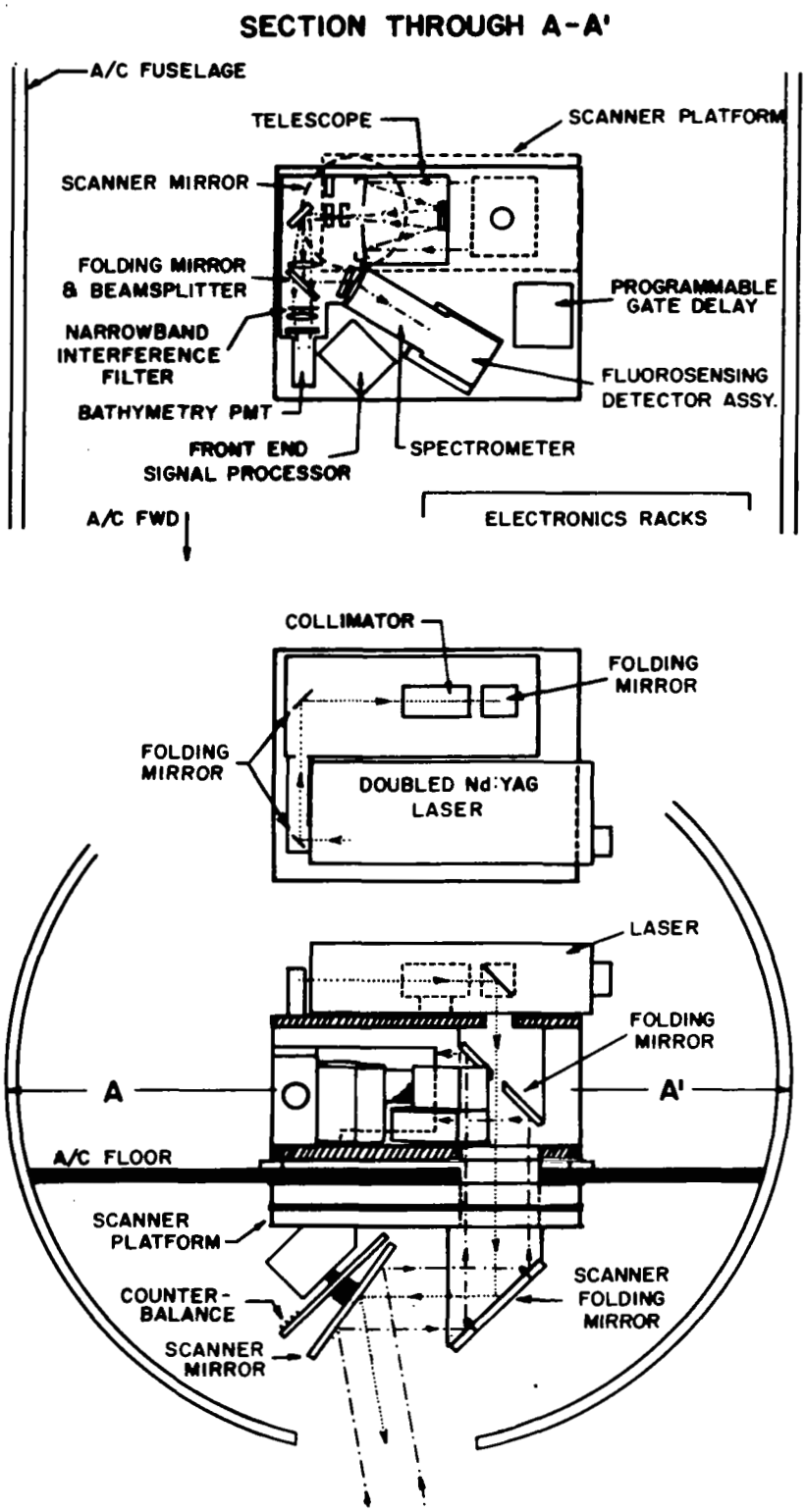

Figure 2.- Detailed view of the transmitter and receiver optics of the AOL system during the Superflux experiments.

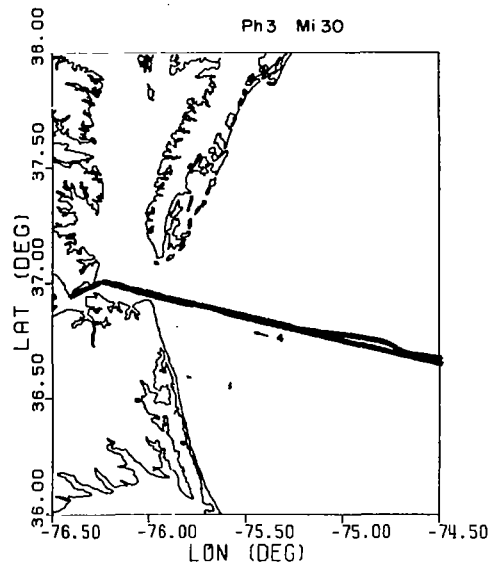

(a) June 20, 1980.

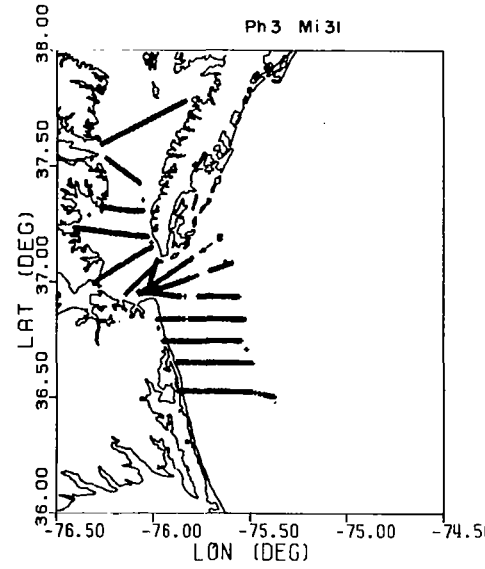

(b) June 23, 1980.

Figure 3.- Computer-drawn ground tracks for flight lines occupied on AOL missions 30 and 31 (June 20 and 23, 1980, respectively).

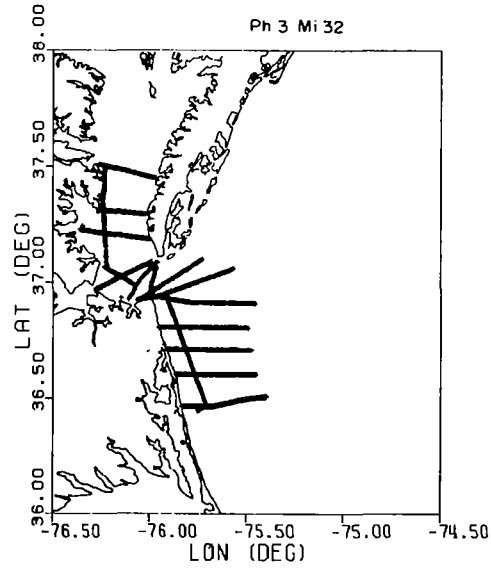

(a) June 25, 1980.

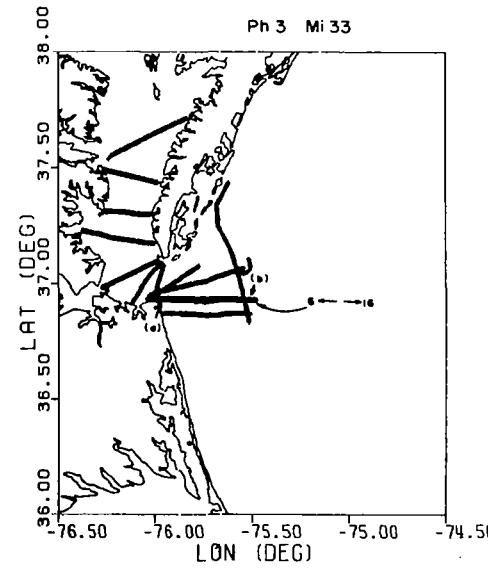

(b) June 27, 1980.

Figure 4.- Computer-drawn ground tracks for flight lines occupied on AOL missions 31 and 32 (June 25 and 27, 1980, respectively).

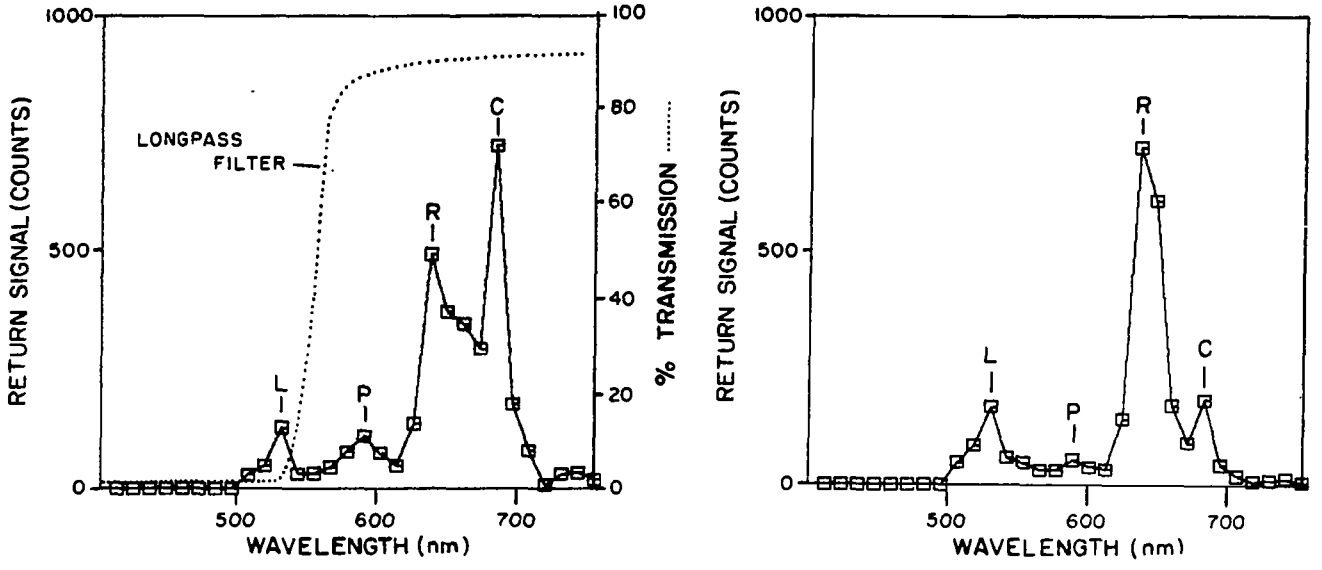

(a) Within the Bay plume.

(b) Offshore.

Figure 5.- Sample AOL spectra from within the Bay plume and offshore. The location of this flight line is given in figure 3(a). P - organic pigments; R - Raman; C - chlorophyll; L - laser.

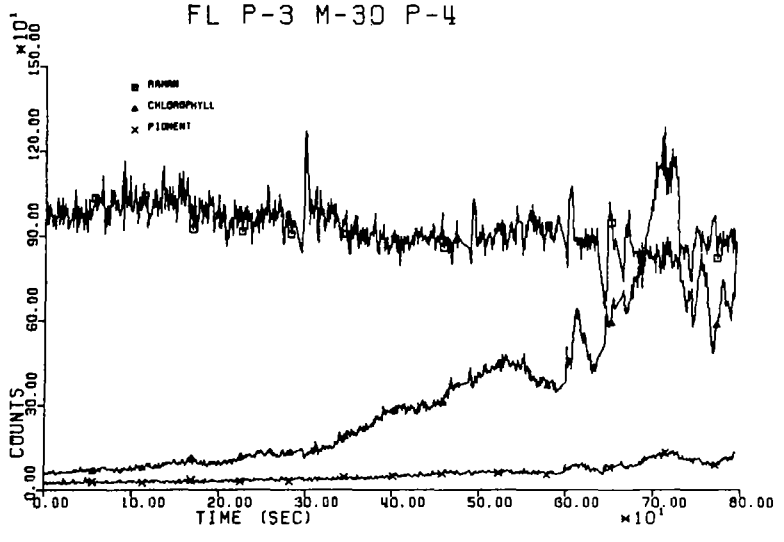

Figure 6.- Sample cross-section from a pass flown on June 23. The location of this flight line is given in figure 3(a).

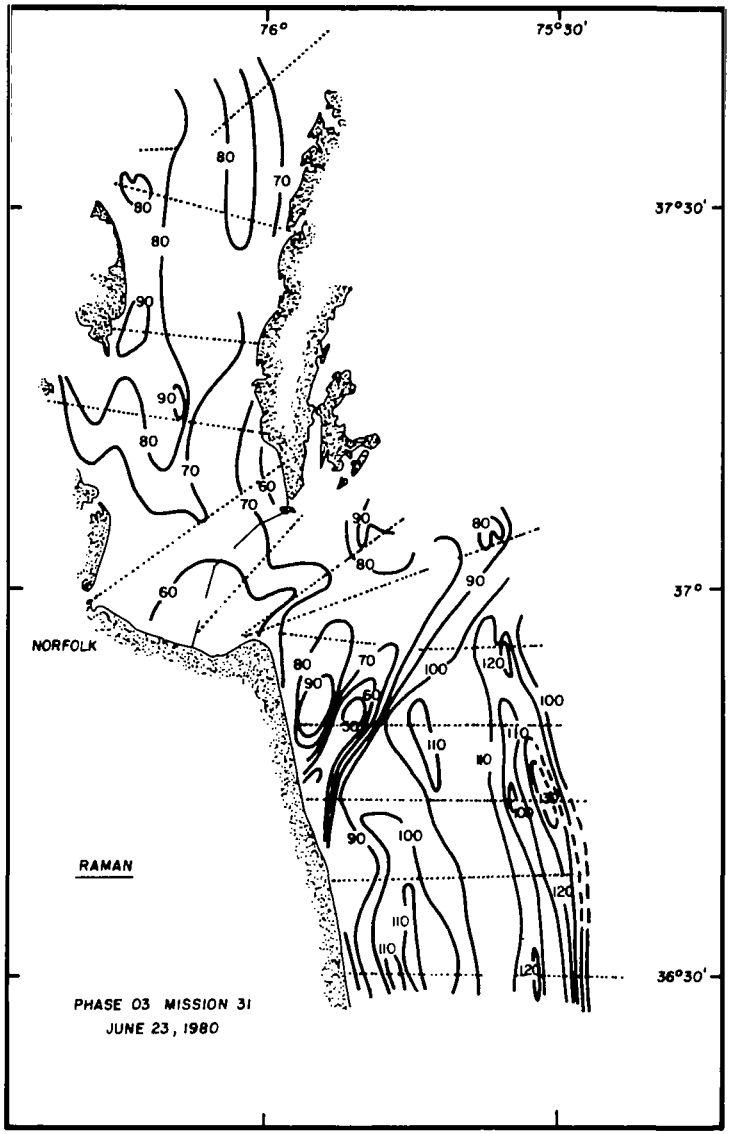

Figure 7.- Contoured plots of relative Raman backscatter from the mission flown on June 23. The dotted segments indicate the ground tracks.

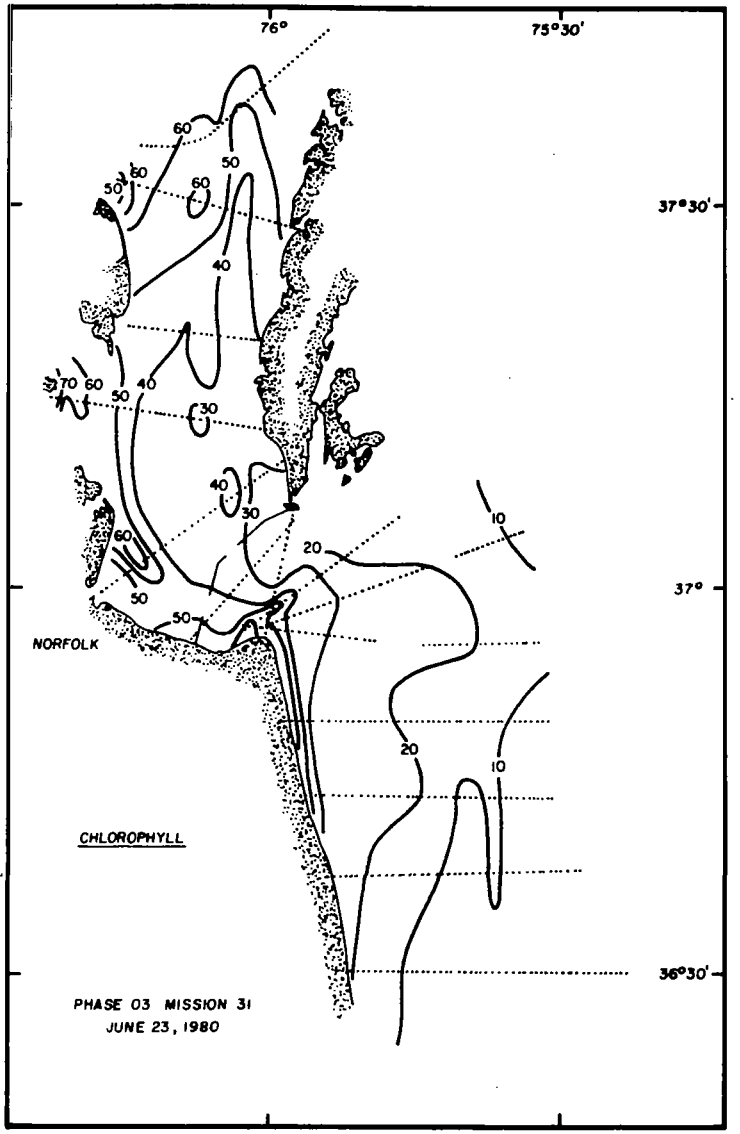

Figure 8.- Contoured plots of relative chlorophyll a fluorescence from the mission flown on June 23.

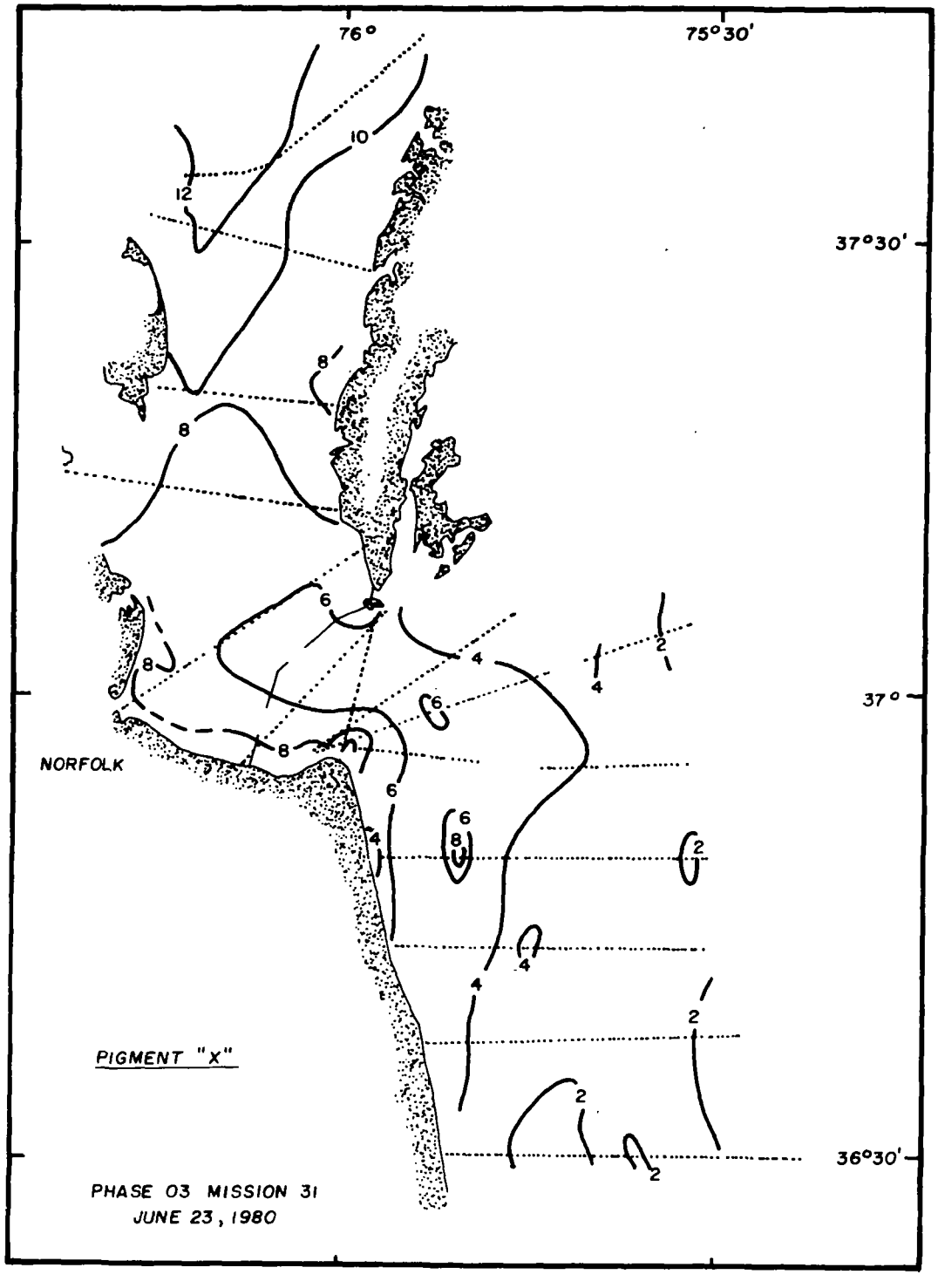

Figure 9.- Contoured plots of relative organic pigment fluorescence from the mission flown on June 23. The organic pigment response has been normalized by the Raman backscatter to remove the effects of spatial variations in water transmissivity.

(a)

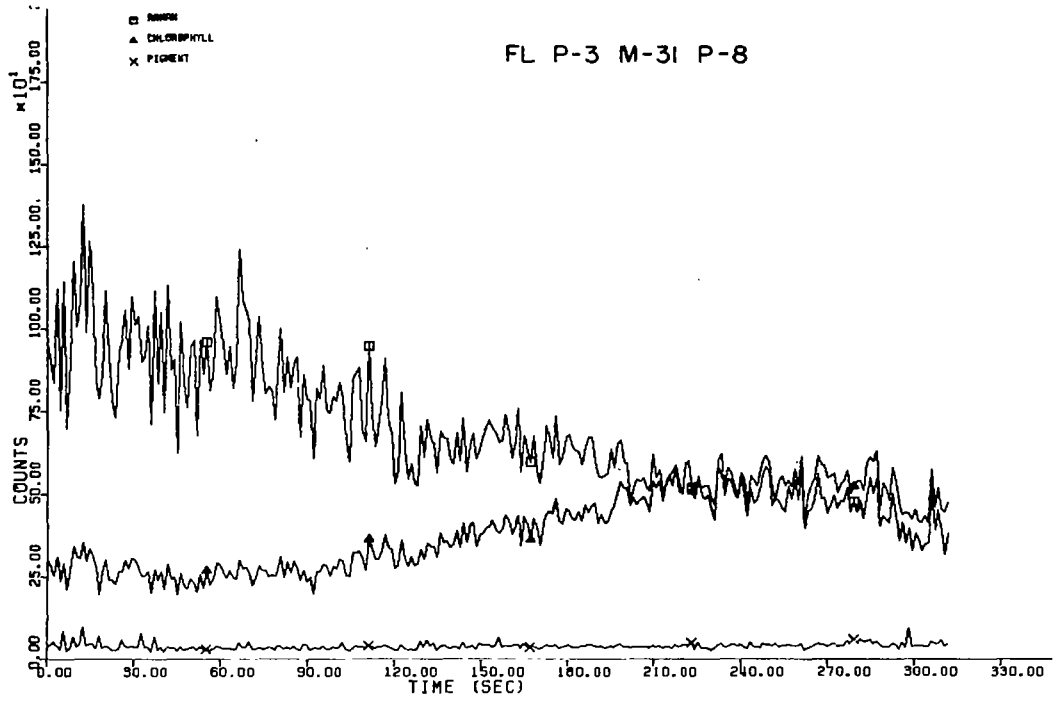

(b)

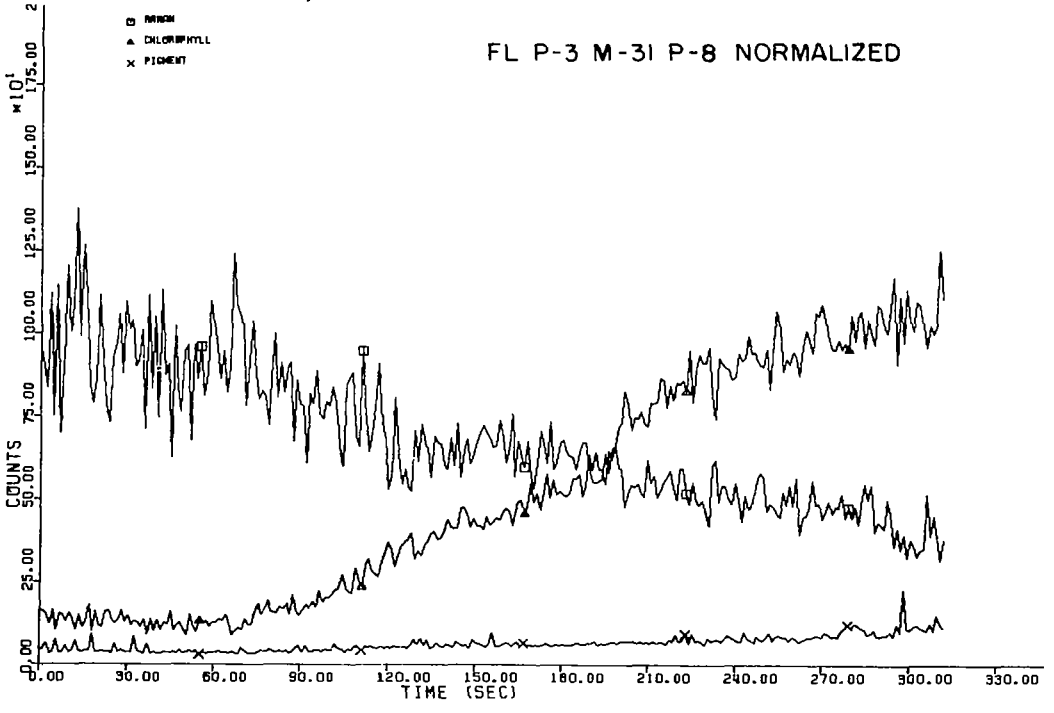

Figure 10.- Comparative cross-sections of flight line 8 from the mission flown on June 23. Figure 10(a) indicates the relative intensities of chlorophyll a and organic pigment fluorescence signals before normalization; the traces in figure 10(b) have been normalized.

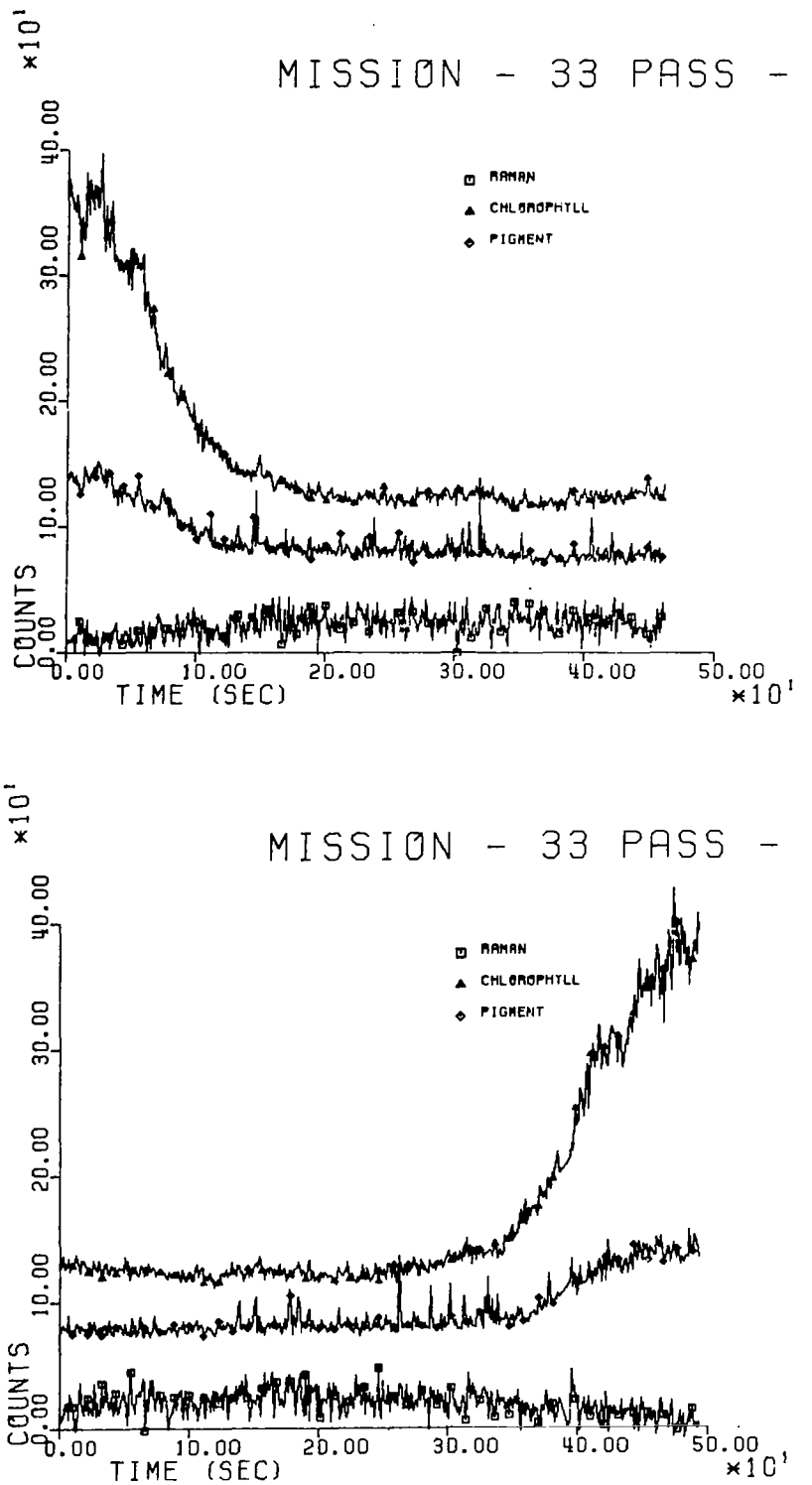

Figure 11.- Comparative cross-sections from flight lines 16 and 6 flown on June 23. Both of these flight lines were taken over the same ground track, but in the opposite direction.

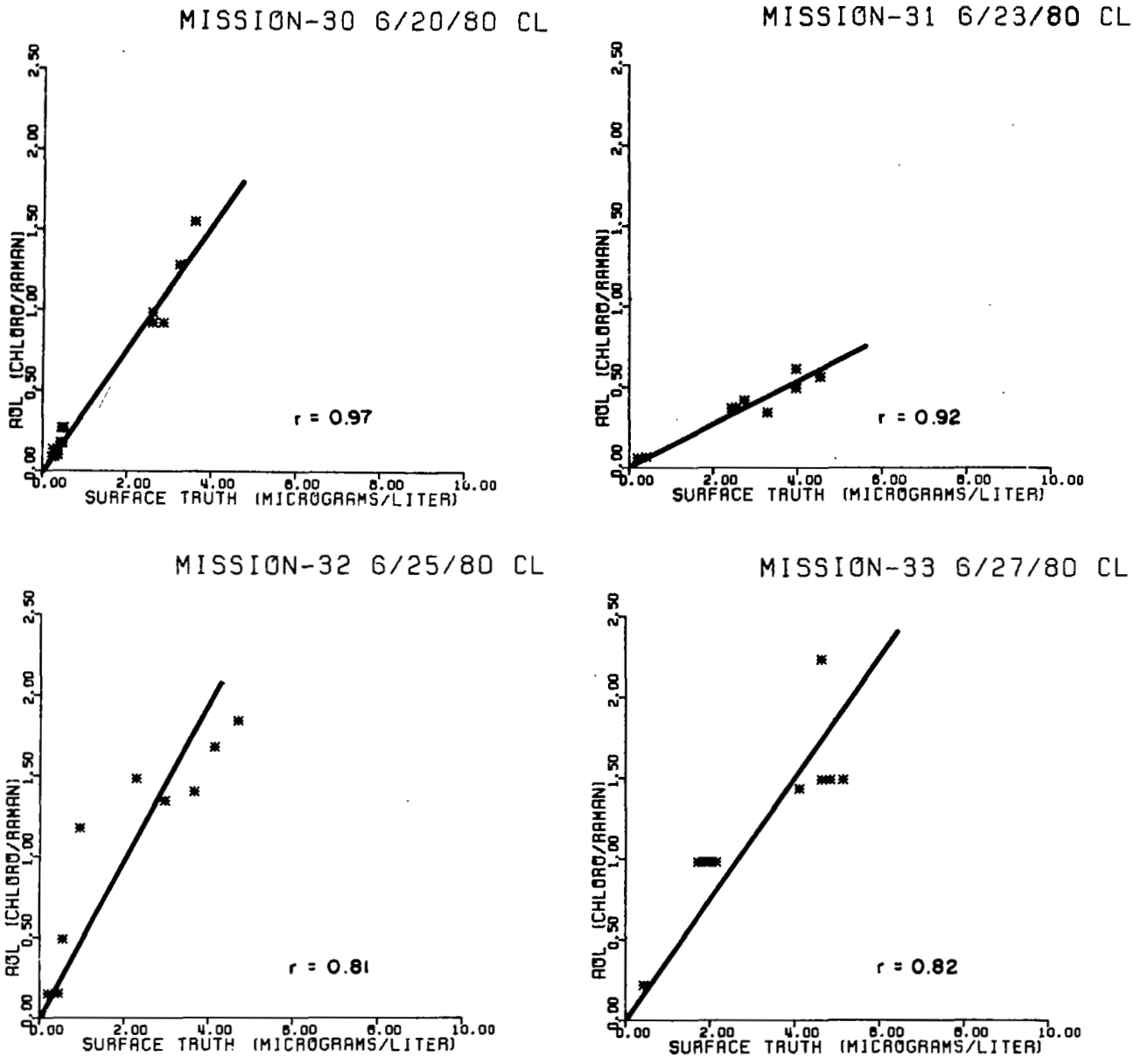

Figure 12.- Comparative plots indicating the agreement between AOL and surface truth chlorophyll a results for the four Superflux missions flown over the Chesapeake Bay mouth in June 1981.

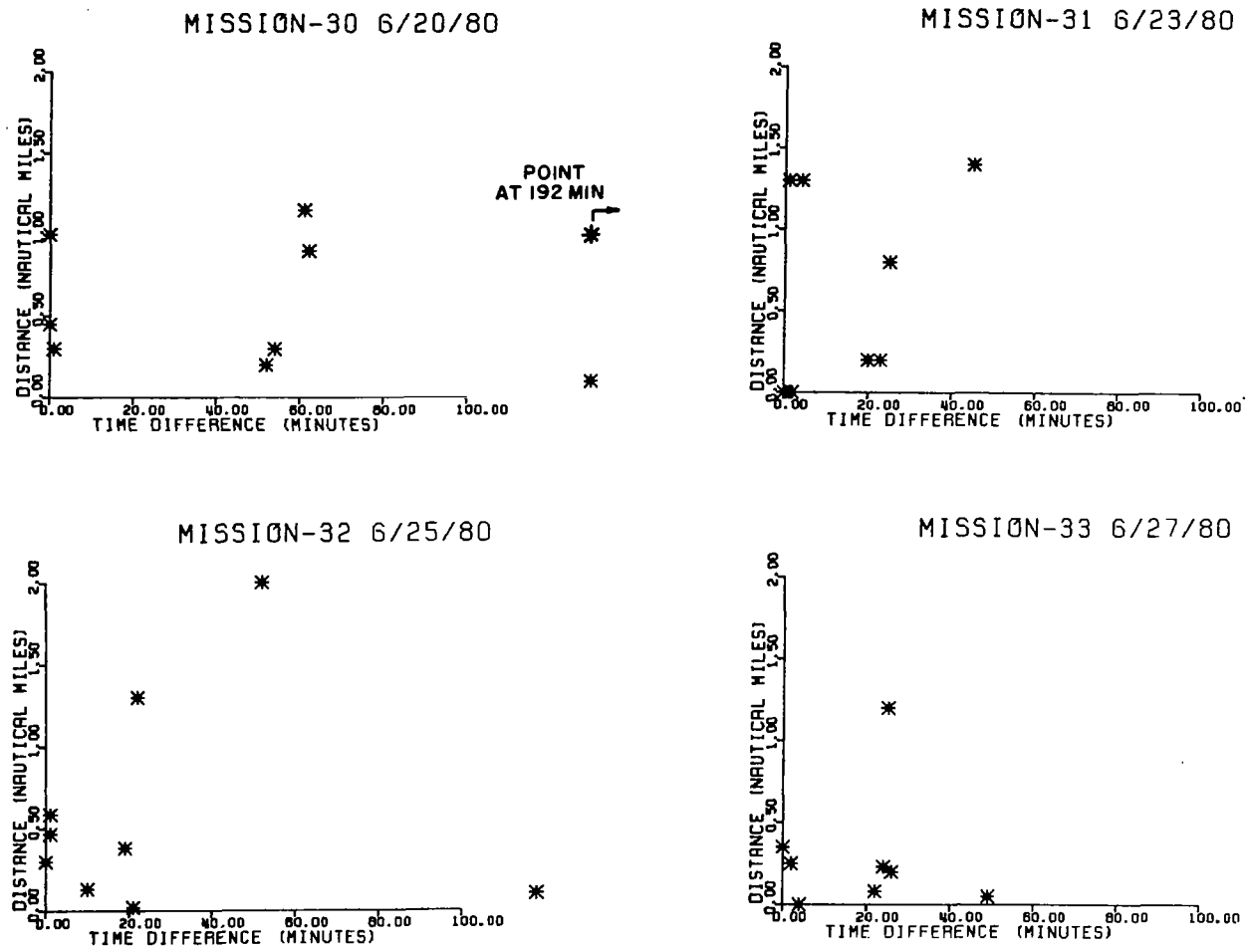

Figure 13.- Plots of temporal and spatial differences between AOL and surface truth sampling for the four Superflux missions flown over the Chesapeake Bay mouth in June 1981.

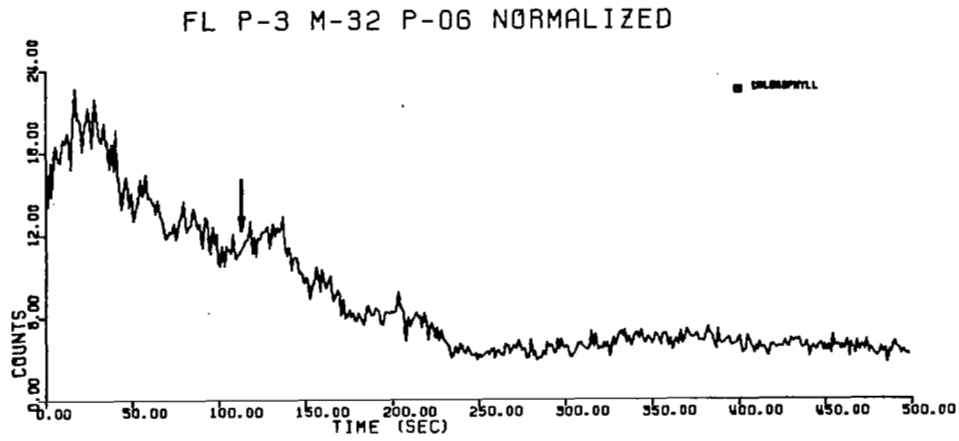

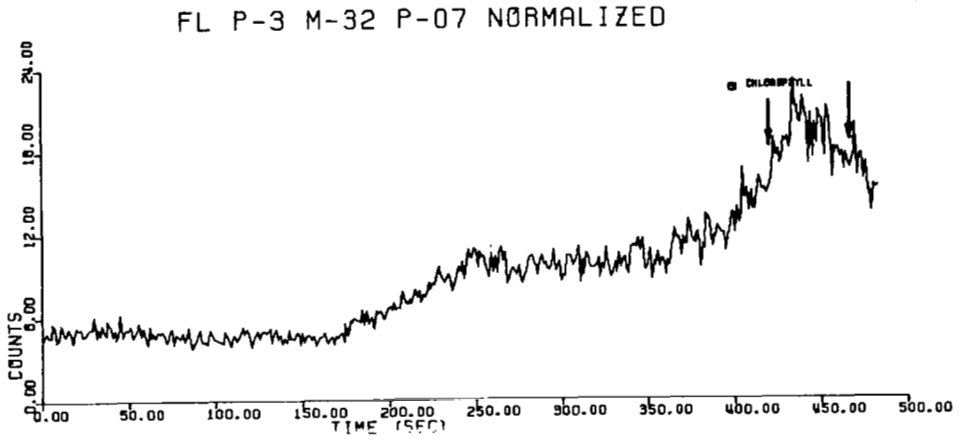

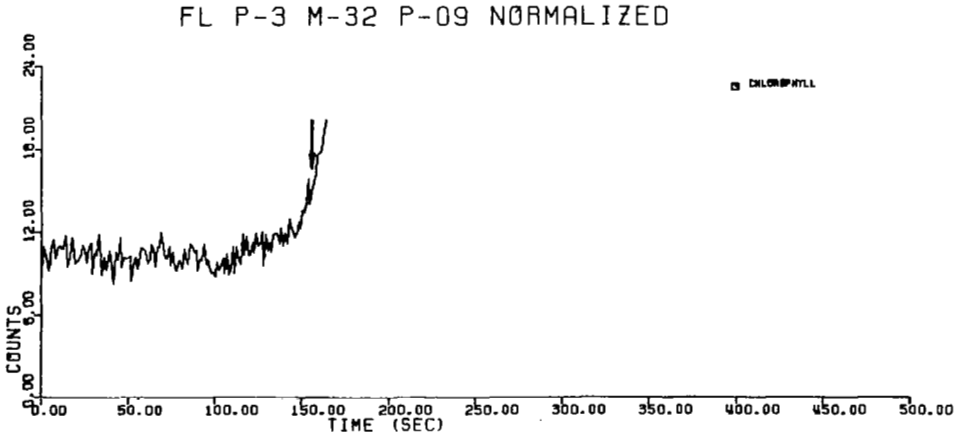

Figure 14.- Cross-sections of normalized chlorophyll a for passes taken on June 25 where surface truth sampling was available. The arrow(s) indicates the location of the high gradient sampling point on each pass.

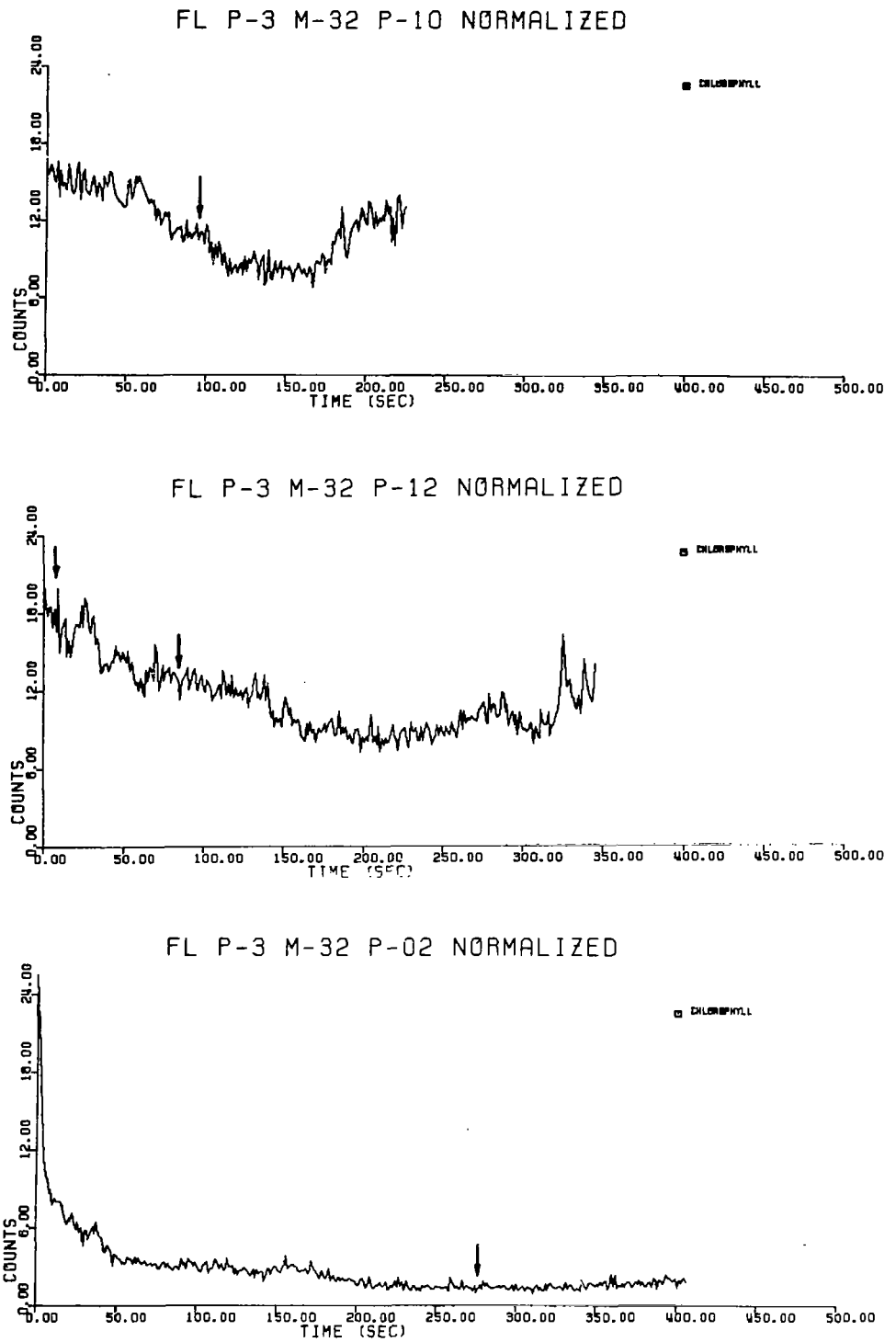

Figure 15.- Cross-sections of normalized chlorophyll a for passes taken on June 25 where surface truth sampling was available. The arrow(s) indicates the location of the low gradient sampling point on each pass.